

Dislocation density on wavefront of a speckle-structure light field

N. B. Baranova, B. Ya. Zel'dovich, A. V. Mamaev, N. F. Pilipetskii, and V. V. Shkunov

Institute of Mechanics Problems, USSR Academy of Sciences

(Submitted 13 May 1982)

Zh. Eksp. Teor. Fiz. 83 1702–1710 (November 1982)

The dislocation density on the wavefront of a speckle-inhomogeneous light field was investigated experimentally as a function of the beam divergence, shape of the angular spectrum, and degree of spatial modulation. The results are in good agreement with the theory.

PACS numbers: 42.20.Cc, 61.70.Jc

In research on coherent optics one encounters, with even increasing frequency, fields that have a speckle structure. One works with such fields in holography^{1–3} and astronomy,⁴ in wave-front-reversal problems,^{5–7} in suppression of self-action in optical amplifiers,^{8,9} and others. The statistical and other diverse properties of speckle fields have been investigated in sufficient detail¹⁰ and their investigation is still continuing.

The term “speckle structure” was coined for spatially inhomogeneous coherent light fields of a special type. The most typical situation that leads to the appearance of speckle fields is realized when a laser wave is reflected from a coarse object whose roughnesses exceed the wavelength in height. The field at a certain observation point is the amplitude sum of a large number of contributions from different points of the surface, with the phases of these contributions having a practically random distribution. By virtue of the central limit theorem of probability theory, such a field has universal (Gaussian) statistics. It is precisely this universal character of the fluctuations of the spotty structure of the field which makes it possible to separate, from the class of all spatially inhomogeneous fields, fields having the indicated statistics, for which the term “speckle field” is now used. We emphasize the importance of the coherence assumption: without it, the contribution of the individual roughnesses would add up without interference, i.e., in intensity. As a result, the overall distribution of the intensity for ordinary (non-laser) illumination is smooth and not spotty.

On the other hand, many studies have been devoted to wave-front dislocations of various non-optical wave fields (see the reviews^{11–13}). In Ref. 14 it was indicated for the first time that wavefront dislocations are possessed by optical fields having a speckle structure. The cited reference contains a detailed theoretical analysis of the properties of the dislocations and their density per unit area was calculated. In Ref. 15 were registered wavefront dislocations of a speckle-inhomogeneous laser wave and the dislocation density was measured for a field with an axisymmetric envelope of the angular spectrum. In the present paper we report the results of experimental investigations of the dislocation density on a wave field as a function of various speckle-field parameters.

1. SOLUTION OF THE WAVE EQUATION NEAR A ZERO OF THE FIELD AMPLITUDE

The difference of a monochromatic beam with high directivity along the z axis

$$E_{\text{real}}(\mathbf{r}, z, t) = \frac{1}{2} [E(\mathbf{r}, z) e^{-i\omega t + ikz} + E^*(\mathbf{r}, z) e^{i\omega t - ikz}] \quad (1)$$

it is correct to use the parabolic equation

$$2ik \frac{\partial E(\mathbf{r}, z)}{\partial z} + \Delta_{\perp} E(\mathbf{r}, z) = 0. \quad (2)$$

Here \mathbf{r} is a two-dimensional vector with components x and y . Assume that at a certain point $\mathbf{r} = 0$ the complex amplitude of the field has an isolated zero $E(0) = 0$. By virtue of the continuity of the field, it can be expanded in powers of the small deflections of \mathbf{r} and z . It is interesting to note that if we confine ourselves to the linear terms of this expansion, the resultant field

$$E(\mathbf{r}, z) = e^{i\alpha} (A_x x + i A_y y) \quad (3)$$

does not depend on z (the null line is directed along the axis) and is an exact solution of the wave equation (2) in all of space. If the directions of the Cartesian axes (x, y) are suitably chosen, A_x and A_y are real. For this solution, the constant-amplitude surfaces are elliptic cylinders with ellipse-axis ratio $|A_y/A_x|$. As for the field phase $\varphi(\mathbf{r}) = \arg E(\mathbf{r})$ it acquires an increment 2π on circling around the zero point. (This can be particularly easily verified for the case $A_x = A_y$, when the solution (3) assumes in cylindrical coordinates the form $A_r \exp[i(\alpha + \varphi)]$). This means that the surface of the wave front, defined by the equation $kz + \varphi(\mathbf{r}, z) = \text{const}$, has at this point a singularity of the screw-dislocation type. Indeed, on circling around zero over the wavefront surface near the dislocation it is easy to go over continuously from one wavefront surface to the next one that differs in phase by 2π .

2. EVOLUTION OF DISLOCATIONS

With continuing diffraction of the speckle-inhomogeneous field along the z axis, the zero-amplitude points describe random snake-like trajectories with characteristic transverse and longitudinal scales λ/θ and λ/θ^2 , respectively, where λ is the wavelength of the radiation and θ is its divergence. These trajectories are not infinite, but start and end at certain points—the points of creation and annihilation of zero pairs. As shown in Ref. 14, the null line can be regarded near these points as a smooth curve. If the angular divergence of the radiation is large, we can simply speak of reversal of the sign of the z component tangent to the smooth curve that defines the zero line. On the contrary, in optics, where the typical divergence is small, it is more appropriate to speak of creation or annihilation of a pair of zeros.

Depending on the relations between the signs of A_x and A_y in the solution (3), which determine the sign of the phase shift $+2\pi$ or -2π on circling around the zero point, the zeros can be positive or negative. It is important to note that dislocations can be created and annihilated only by zeros of opposite sign, so that the dislocation trajectories are start out and terminate only at points where trajectories of dislocations of opposite signs coalesce.

3. POINTS OF APPEARANCE OF INTERFERENCE FRINGES

The question now arises whether it is possible to record in experiment the zeros of the amplitudes and the corresponding wavefront dislocations. The usual methods of measuring the field intensity will not do for this purpose, since they are of limited accuracy and cannot distinguish a point with zero intensity from one with a very low intensity.

We consider the interference pattern produced in the plane $z = 0$ by superposition of a smooth reference field, say a plane wave $\exp(iqx)$, and a field with dislocation of type (3)

$$I(r, \varphi) \sim |e^{iqr \cos \varphi} + re^{i\varphi}|^2 = 1 + r^2 + 2r \cos(\varphi + qr \cos \varphi). \quad (4)$$

Figure 1a shows the interference pattern determined by relation (4). The solid lines show the crests of the interference fringes, and the dashed their troughs. It can be seen that a dislocation of type (3) corresponds on the interference pattern to a point where an interference fringe appears. The cases dark or light fringes as well as all the intermediate situations have different phase shifts for the wave with dislocation and for the smooth reference wave at the zero-amplitude point. Figure 1b shows for comparison a section of the interference pattern of a speckle-inhomogeneous laser beam with a plane wave as the reference.

4. DISLOCATION DENSITY IN A SPECKLE FIELD WITH TOTAL SPATIAL MODULATION

a. Calculation of dislocation density from the form of the angular spectrum

To calculate the density of the zeros (meaning also of the dislocations) in a speckle-inhomogeneous field with Gaussian statistics we can proceed as follows. The total number NS of the zeros in a certain region of the (x, y) plane with area S is expressed in the form

$$NS = \left\langle \int dx dy \delta[E_1(x, y)] \delta[E_2(x, y)] \left| \frac{\partial(E_1, E_2)}{\partial(x, y)} \right| \right\rangle. \quad (5)$$

Here $E(x, y) = E_1(x, y) + iE_2(x, y)$, the angle brackets denote averaging over the ensemble of the random fields, and $\delta(E)$ is the Dirac δ function. The validity of this expression can be easily verified by noting that each zero point of the total field makes (prior to the averaging) a unity contribution to the right-hand side of the equation. Since a Jacobian $|\partial(E_1, E_2)/\partial(x, y)|$ containing spatial derivatives of the fields is present in the integral (5), the averaging in (5) must be carried out using the joint probability density W_6 of the quantities E_1 and E_2 and of their gradients at the given point. As a result we obtain

$$N = \int \left| \frac{\partial(E_1, E_2)}{\partial(x, y)} \right| W_6 \left(0, 0, \frac{\partial E_1}{\partial x}, \frac{\partial E_2}{\partial x}, \frac{\partial E_1}{\partial y}, \frac{\partial E_2}{\partial y} \right) d \left(\frac{\partial E_1}{\partial x} \right) \dots d \left(\frac{\partial E_2}{\partial y} \right). \quad (6)$$

For fields with Gaussian statistics, W_6 can be expressed in terms of a complex-field correlator defined in terms of the normalized angular spectrum of the investigated field

$$\langle E^*(\mathbf{r}_1) E(\mathbf{r}_2) \rangle = I \int j(\theta) e^{ik\theta(r_2 - r_1)} d^2\theta, \quad \int j(\theta) d^2\theta = 1. \quad (7)$$

After a number transformation we obtain after integrating in (6) (see Ref. 14)

$$N = (2\pi/\lambda^2) (\det C)^{1/2}; \quad C_{ik} = \overline{\theta_i \theta_k} - \overline{\theta_i} \overline{\theta_k}. \quad (8)$$

Here λ is the radiation wavelength

$$\overline{\theta_i} = \int \theta_i j(\theta) d^2\theta, \quad \overline{\theta_i \theta_k} = \int \theta_i \theta_k j(\theta) d^2\theta.$$

By suitable choice of the axis (by a shift on the (θ_x, θ_y) plane and by selecting the orientations of the coordinate axes x and y we can diagonalize the matrix C_{ik} . Then

$$N = (2\pi/\lambda^2) (\overline{\theta_x^2} \overline{\theta_y^2})^{1/2}. \quad (9)$$

The quantities $\overline{\theta_{x,y}^2}$ characterize the divergence of the beam with respect to the corresponding coordinates. The speckle-field dislocation density is thus of the order of the speckle-spot density $\sim (\theta/\lambda)^2$, where θ is the field divergence. The numerical value for the density is determined by the form of the angular spectrum $j(\theta)$ of the field.

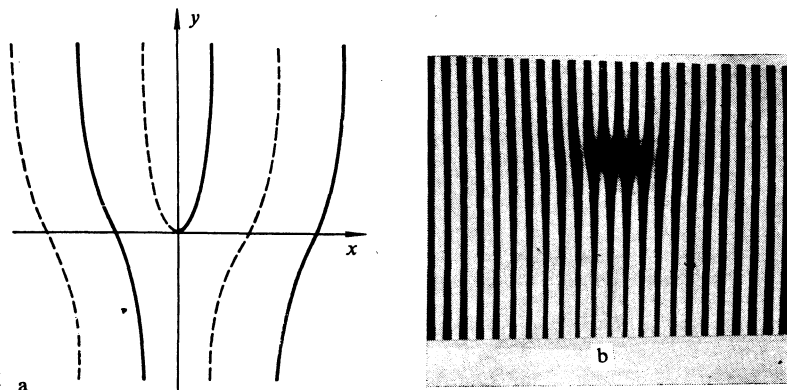


FIG. 1. Interference pattern of a field with a wave-front dislocation, for a plane reference wave: a—theoretical calculation, b—magnified photograph of a section of the speckle-field interference pattern.

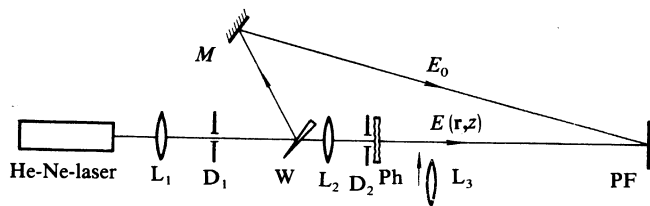


FIG. 2. Experimental setup for the investigation of the dislocation density for different speckle-field angle spectra: D_2 —diaphragm of variable shape and dimensions, L_1 and L_2 —telescope lenses, D_1 —spatial filter. The lens L_3 was used in investigations of the growth dynamics of the dislocation density to project different sections of the beam behind the phase plate Ph on the plane of the photographic film PF, W—optical wedge.

b. Measurement of the dislocation density

The experimental setup is shown in Fig. 2. A single-mode linearly polarized beam of an He-Ne laser was split

into two-reference E_0 and signal $E(r,z)$. The single beam was widened with a telescope to a diameter ≈ 4.7 mm and was passed through a diaphragmed phase plate Ph (standard for experiments on wave-front reversal⁵). The signal beam acquired as a result phase distortions, but the amplitude of the wave within the confines of the diaphragm remained practically constant. The phase plate was strong enough to prevent a regular component from being prominent in the distorted wave. The total radiation divergence at the e^{-1} level was $\Delta\theta = 6.7 \times 10^{-3}$ rad. In the course of propagation the phase modulation in the signal beam was transformed into amplitude modulation: the beam acquired a speckle structure. The reference and signal beams interfered on a photographic film PF located at a distance ≈ 9.5 m away from the phase plate.

Figure 3 shows photographs: (a) of a section of the speckle picture of the signal wave $E(r,z)$, (b) of the same section but modulated by interference with the wave E_0 . The

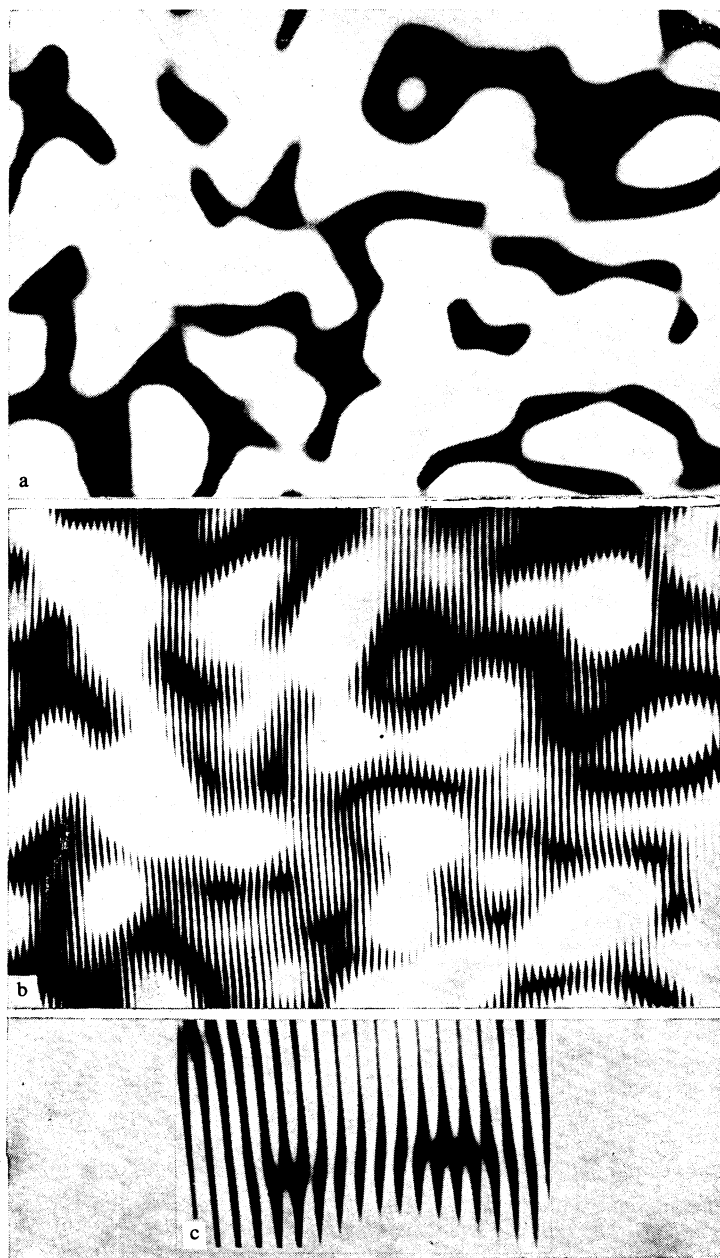


FIG. 3. Section of the speckle picture of the signal wave (a) and the corresponding interference pattern (b); Fig. c shows two dislocations of opposite sign.

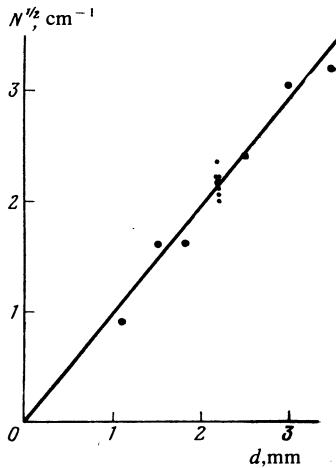


FIG. 4. Dependence of $N^{1/2}$ on the diameter of the round diaphragm D_2 .

points at which the interference fringes appear correspond to dislocations of the wave front and, by the same token, to zeros of the amplitude $E(\mathbf{r}, z)$. By comparing these photographs we can verify that a zero amplitude exists not at all minima of the speckle picture. Figure 3c shows a magnified section of the photograph with two dislocations of opposite sign.

To measure the dislocation density N [cm^{-2}] of the speckle field we counted the number of points at which interference fringes were produced on a 2.3×3.4 cm film frame. The irregular speckle divergence θ_0 and the form of the angular spectrum $j(\theta)$ of the field $E(\mathbf{r}, z)$ in the plane of the frame were determined by the angle of view and by the shape of the diaphragm.

For a round diaphragm of diameter d we have $\theta_0 = d / 2R$ as well as $j(\theta) = 1/\pi\theta_0$ at $|\theta| \leq \theta_0$ and $j(\theta) = 0$ at $|\theta| > \theta_0$. For such an angular spectrum we obtain from (9) $N = \pi\theta_0^2 / 2\lambda^2$.

Figure 4 shows the experimental points of the dependence of $N^{1/2}$ on d . The scatter of the values of $N^{1/2}$ at a diameter $d = 2.2$ mm is shown for different realizations of the speckle picture. The solid straight line is a plot of the theoretical relation (9).

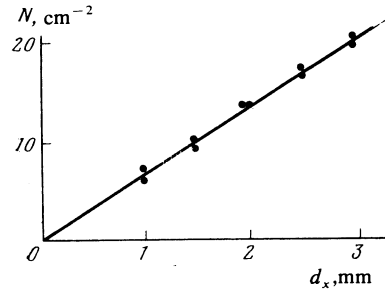


FIG. 6. Dislocation density N vs distance z from phase plate, for two plates of different strength.

For a rectangular diaphragm with unequal x and y , the angular spectrum $f(\theta)$ is asymmetric: $j(\theta) = 1/4\theta_0^x \theta_0^y$ at $|\theta_x| \leq \theta_0^x$, $|\theta_y| \leq \theta_0^y$ and $j(\theta) = 0$ at $|\theta_x| > \theta_0^x$, $|\theta_y| > \theta_0^y$. The speckle picture is stretched out in this case in the direction corresponding to the smaller divergence (Fig. 5). In the experiment, the diaphragm dimension d_y , along one of the coordinates remained constant. The experimental points $N(d_x)$ and the corresponding linear dependence calculated from Eq. (9) are shown in Fig. 6. The results (Figs. 5 and 6) point to a good agreement for both the functional relations and the absolute values obtained theoretically and in experiment.

c. Dynamics of dislocation-density buildup

As already noted, the wavefront dislocation points coincide with the points where the speckle field amplitude vanishes. The speckle-inhomogeneous wave has directly behind the phase plate a spatial modulation of pure phase type. There are therefore in this region no amplitude zeros, meaning also no wavefront dislocations. The dislocation density increases and reaches a stationary value as the signal-wave amplitude modulation develops.

In the experiment, the lens L_3 (see Fig. 2) projected into the region of interference with the reference wave the various sections of the signal beam behind the phase plate. The dislocation density was measured for phase plates of different strengths and producing different irregular divergence $\Delta\theta$ of the distorted radiation. The experimental dependence of the dislocation density on the distance z to the phase plate

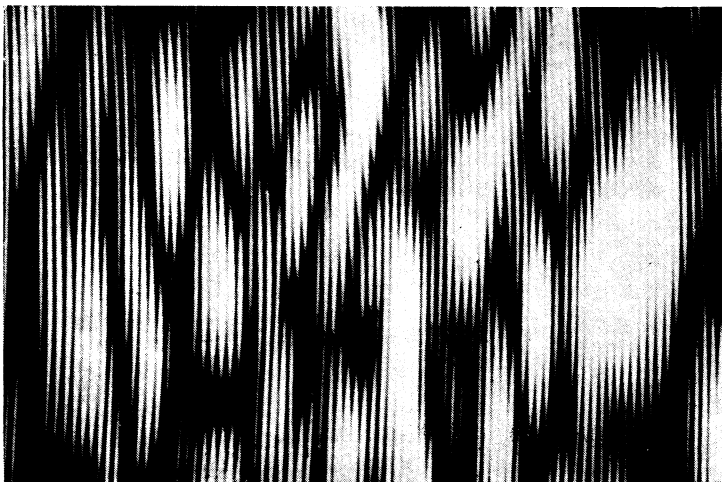


FIG. 5. Interference pattern of field with asymmetric angular spectrum.

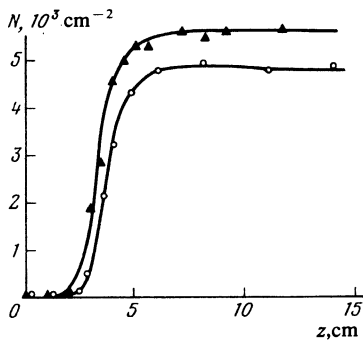


FIG. 7. Buildup of dislocation density N with increasing distance z from the phase plate for two plates of different strength.

is shown in Fig. 7. The dislocation density builds up with increasing distance from the phase plate and assumes abruptly a stationary value $N \sim 2\pi(\Delta\theta)^2/\lambda^2$ at distances $z \sim \lambda(\Delta\theta)^2$ corresponding to the Fresnel length of the speckle-field of the divergence $\Delta\theta$. The larger the divergence $\Delta\theta$, the larger the stationary dislocation density and the faster the dislocation density reaches a stationary value.

5. WAVEFRONT DISLOCATIONS IN A SPECKLE FIELD WITH INCOMPLETE SPATIAL MODULATION

A speckle field with incomplete spatial modulation is produced upon superposition of an irregular field from a random source on a regular component that is coherent with this source. Fields of this type are typical of cases when the regular field passes through a weakly distorting medium.¹⁶ Turbulent distortions in a weak-fluctuation regime¹⁷ lead in atmospheric optics to fields with incomplete spatial modulation.

If a speckle-inhomogeneous field $E_1(r,z)$ with average intensity $\langle I \rangle$ is mixed with a regular (plane or spherical) wave E_2 of intensity I_r , the dislocations of the wavefront of the combined field are produced at points where $E_1(r,z) = -E_2(r,z)$. If the modulus of the regular component in the region of interest to us is constant, $|E_2(r,z)| = I_r^{1/2} = \text{const}$, it is easy to calculate the dislocation density also in this case. Indeed, the probability density for a field $E_1(r,z)$ with Gaussian statistics to assume a value $-E_2(r,z)$ is proportional to $\exp(-|E_2|^2/\langle I \rangle)$. Therefore the dislocation density per unit area of a field with incomplete spatial modulation is given by

$$N = N_0 \exp(-I_r/\langle I \rangle). \quad (10)$$

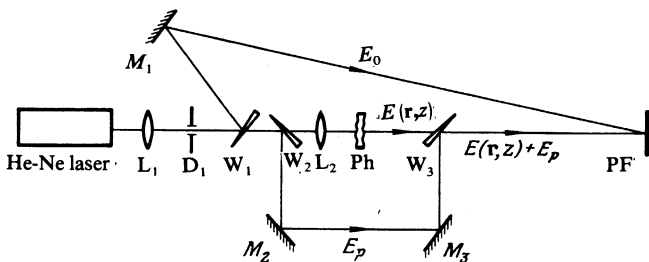


FIG. 8. Experimental setup for the measurement of the dislocation density of fields with incomplete spatial modulation. An additional regular component E_p was mixed with the signal wave by means of mirrors M_2 , M_3 and wedges W_2 , W_3 .

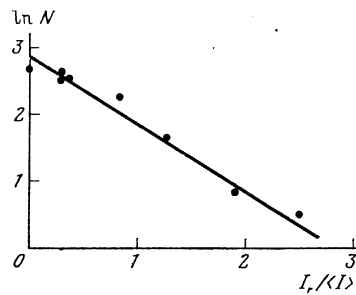


FIG. 9. Experimental points of the dislocation density $\ln N$ vs the ratio $I_r/\langle I \rangle$ of the intensities of the regular and irregular components of the signal wave with incomplete spacial modulation, as well as the corresponding theoretical straight-line plot of Eq. (10).

Here N_0 is the dislocation density of the speckle-inhomogeneous part of the field.

In the experiment (Fig. 8), an additional spherical wave, localized within the same solid angle as the reference wave, was directed into the region of interference with the latter. The experimental points and the theoretical relation (10) for the dislocation density as functions of $I_r/\langle I \rangle$ are shown in Fig. 9. This diagram, too, illustrates the good agreement between theory and experiment.

6. CONCLUSION

The investigation of the wavefront dislocations is important from the conceptual point of view, since it is sometimes more useful to have a correct picture than to know the exact equations. In addition, the presence of dislocations must be taken into account in modern technical facilities. Thus, it can be firmly asserted that it is impossible to reverse a field wavefront with dislocation with the aid of flexible adaptive mirrors.¹⁶ To reverse a wavefront with a mirror it is necessary that the constant-phase surface of the light field coincide with the surface of the mirror. Understandably, it is impossible to bend a mirror continuously to make it duplicate the form of the wavefront near a dislocation. It is therefore of great interest to investigate additive-optics problems with account taken of the wavefront dislocations.

The authors thank A. L. Gyulamiryan for help with the work, and A. I. Arnol'd, I. E. Dzyaloshinskii, and I. I. Sobel'man for useful discussions.

¹E. Archbold and A. Ennas, *Optica Acta* **19**, 253 (1972).

²N. G. Vlasov and A. E. Shtan'ko, *Opt. Spektrosk.* **43**, 192 (1977).

³V. V. Shkunov and Y. B. Zel'dovich, *Appl. Opt.* **18**, 3633 (1979).

⁴A. A. Tokovinin and P. V. Shcheglov, *Usp. Fiz. Nauk* **129**, 645 (1979) [*Sov. Phys Usp.* **22**, 960 (1979)].

⁵B. Ya. Zel'dovich, V. I. Popovichev, V. V. Ragul'skii, and F. S. Faizulov, *Pis'ma Zh. Eksp. Teor. Fiz.* **15**, 160 (1972) [*JETP Lett.* **15**, 109 (1972)].

⁶V. N. Blashchuk, B. Ya. Zel'dovich, and V. V. Shkunov, *Kvant. Elektron. (Moscow)* **7**, 2559 (1980) [*Sov. J. Quantum Electron.* **10**, 1494 (1980)].

⁷O. L. Kulikov, N. F. Pilipetskii, A. N. Sudarkin, and V. V. Shkunov, *Pis'ma Zh. Eksp. Teor. Fiz.* **31**, 377 (1980) [*JETP Lett.* **31**, 345 (1980)].

⁸V. I. Kryzhanovskii, A. A. Mak, V. A. Serebryakov, and V. E. Yashin, *Pis'ma Zh. Tekh. Fiz.* **7**, 400 (1981) [*Soviet Tech. Phys. Lett.* **7**, 176 (1981)].

⁹B. Ya. Zel'dovich and T. V. Yakovleva, *Kvant. Elektron. (Moscow)* **7**, 1325 (1980) [*Sov. J. Quantum Electron.* **10**, 757 (1980)].

¹⁰*Laser Speckle and Related Phenomena (Topics in Appl. Phys.)*, Springer, 1975.

- ¹¹M. V. Berry, J. F. Nye, and F. J. Wright, *Phil. Trans. London A*-**291**, 454 (1979).
- ¹²J. Nye and M. V. Berry, *Proc. Roy. Soc. London A*-**336**, 165 (1974).
- ¹³F. J. Wright, in: *Structural Stability in Physics*, W. Gütting and H. Eikemeir, eds. Springer, 1979.
- ¹⁴N. B. Baranova and B. Ya. Zel'dovich, *Zh. Eksp. Teor. Fiz.* **80**, 1789 (1981) [*Sov. Phys. JETP* **53**, 925 (1981)].
- ¹⁵N. B. Baranova, B. Ya. Zel'dovich, A. V. Mamaev, N. F. Pilipetskii, and

- V. V. Shkunov, *Pis'ma Zh. Eksp. Teor. Fiz.* **33**, 206 (1981) [*JETP Lett.* **33**, 195 (1981)].
- ¹⁶B. Ya. Zel'dovich and V. V. Shkunov, *Kvant. Elektron. (Moscow)* **4**, 2353 (1977) [*Sov. J. Quantum Electron.* **7**, 134S (1977)].
- ¹⁷Special Issue of *JOSA on Adaptive Optics*, *JOSA*, **67**, No. 3 (1977).

Translated by J. G. Adashko